Theory of traveling filaments in bistable semiconductor structures

Pavel Rodin*
Institut für Theoretische Physik, Technische Universität Berlin, Hardenbergstrasse 36, D-10623, Berlin, Germany
and Ioffe Physicotechnical Institute of Russian Academy of Sciences, Politechnicheskaya 26, 194021, St. Petersburg, Russia
(Received 7 May 2003; revised manuscript received 29 September 2003; published 12 January 2004)

We present a generic nonlinear model for current filamentation in semiconductor structures with S-shaped current-voltage characteristics. The model accounts for the Joule self-heating of a current density filament. It is shown that the self-heating leads to a bifurcation from static to traveling filaments. Filaments start to travel when an increase of the lattice temperature has a negative impact on the cathode-anode transport. Since the impact ionization rate decreases with temperature, this occurs for a wide class of semiconductor systems whose bistability is due to the avalanche impact ionization. We develop an analytical theory of traveling filaments which reveals the mechanism of filament motion, finds the condition for bifurcation to traveling filament, and determines the filament velocity.

DOI: 10.1103/PhysRevB.69.045307 PACS number(s): 72.20.Ht, 85.30.−z, 05.65.+b

I. INTRODUCTION

Bistable semiconductor systems with S-shaped current-voltage characteristics exhibit a spontaneous formation of current density filaments — high current density domains in a low current density environment.[1–6] Current filamentation typically develops due to the spatial long wavelength instability — known as Ridley instability[1] — of the uniform state with a negative differential conductance when the device is operated via sufficiently large load resistance[7,8] (Fig. 1). The formation of current filaments potentially leads to a thermal destruction of the semiconductor structure, and thus is an important scenario for semiconductor device failure.[4,6] Current filaments have been studied in bulk semiconductors,[2,5,9,10] thin semiconductor films,[11–15] and layered structures of semiconductor devices.[16–21] Over the last decade, the focus has been shifted from static filaments to complex spatiotemporal dynamics of current density patterns.[22–25] Modern experimental techniques based on scanning electron microscopy,[26] detection of infrared radiation,[27] and interferometric mapping[28] provide means for a direct observation of current density dynamics during filamentation. With regard to pattern formation and nonlinear phenomena, bistable semiconductors have much in common with other spatially distributed active media such as gas discharge systems or chemical and biological systems.[22,29–33]

Apart from the well understood bifurcation which leads to temporal periodic or chaotic oscillations,[34–37] static filaments may undergo a secondary bifurcation that leads to traveling filaments. A lateral movement of filaments along the device has been observed experimentally for different types of semiconductor structures.[27,28,38,39] Remarkably, in all these structures the S-shaped characteristic is associated with avalanche impact ionization. Since impact ionization coefficients decrease with temperature at high electrical fields,[4] the onset of filament motion has been attributed to the self-heating of the filament[40]: the filament is expected to migrate to a colder region as the temperature at its initial location increases. When current filamentation is unavoidable, the migration is desirable in applications because the filament motion delocalizes the heating of the semiconductor structure and thus reduces the hazard of thermal destruction.

The purposes of this paper are to describe the mechanism of filament motion, to develop a generic nonlinear model for traveling filament, to find the condition for bifurcation to traveling filament, and to determine the filament velocity. We demonstrate that the transition from static to traveling filaments due to Joule self-heating represents a generic effect which potentially appears in any bistable semiconductor structure provided that transport in the cathode-anode direction is sensitive to temperature.

II. MODEL OF A BISTABLE SEMICONDUCTOR SYSTEM

For many semiconductors and semiconductor devices current filamentation can be described by a two-component reaction-diffusion model which consists of a partial differential equation for the bistable element and an integrodifferential Kirchhoff equation for the external circuit[7,8,41]:

$$\frac{\partial a}{\partial t}=\nabla_\perp(D_a(a)\nabla_\perp a)+f(a,u),\quad \nabla_\perp\equiv\mathbf{e}_x\partial_x+\mathbf{e}_y\partial_y, \qquad (1)$$

$$\tau_u\frac{du}{dt}=U_0-u-R\int_S J(a,u)dxdy,\quad \tau_u\equiv RC. \qquad (2)$$

Here the variable $a(x,y,t)$ characterizes the internal state of the device and the variable $u(t)$ is the voltage over the device, U_0 is the total applied voltage, J is the current density, R is the load resistance connected in series with the device, C is the effective capacitance of the device and the external circuit, and S is the device cross section (Fig. 1). The local kinetic function $f(a,u)$ and the $J(a,u)$ dependence contain all the information about transport in the cathode-anode (vertical) direction; the diffusion coefficient $D_a(a)$ characterizes lateral coupling in the spatially extended element. In the bistability range $u_h<u<u_{th}$ (see Fig. 1) the local kinetic function $f(a,u)$ has three zeros a_{off}, a_{int}, and a_{on} corresponding to the off, intermediate, and on branches of the current voltage characteristic. It has one zero outside the bistability range. For the homogeneous state, the local dependence $a(u)$ is calculated from $f(a,u)=0$, and then inserted into $J(a,u)$

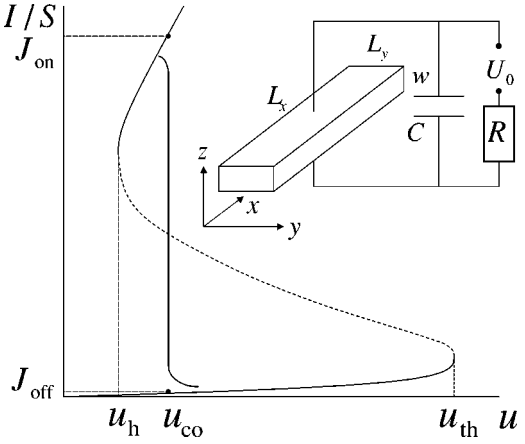

FIG. 1. Current density vs voltage characteristic of a bistable structure. The average current density I/S is shown, where $S=L_xL_y$ is the cross section of the structure. An unstable middle branch with negative differential conductance is depicted by the dashed line. The hold and threshold voltages are denoted as $u_{\rm h}$ and $u_{\rm th}$, respectively. The vertical branch at $u=u_{\rm co}$ corresponds to a static filament. The inset shows a sketch of a bistable semiconductor structure operated in the external circuit with load resistance R, capacitance C, and bias U_0.

in order to determine the local current-voltage characteristic $J(u)\equiv J(a(u),u)$. Typically, $\partial_u f,\partial_a J,\partial_u J>0$. The model (1), (2) belongs to a class of activator-inhibitor models with global inhibition.[25] Variables a and u serve as the activator and inhibitor, respectively. The time scale of the activator a is $\tau_a=\partial_a f^{-1}$.[7] Specific functional forms $f(a,u)$, $J(a,u)$, and $D_a(a)$ have been derived for various semiconductors and semiconductor structures.[2,7–10,17,18,20,34,41,42] The physical meaning of a depends on the particular type of bistable structure: a corresponds to the bias of the emitter p-n junction for avalanche transistors,[18] thyristors,[20] and thyristorlike structures,[21] the interface charge for heterostructure hot electron diodes,[34] the electron charge stored in the quantum well for bistable double barrier resonant tunneling diodes,[41,42] etc.

The two-component model (1), (2) are capable of describing steady filaments[8] as well as the temporal oscillation of current density filaments.[34,36,37] However, its solutions do not include traveling filaments.

The self-heating of the filament has an impact on filament dynamics when vertical transport is sensitive to temperature. In terms of Eq. (1) this means that the local kinetic function f depends on the lattice temperature T. We get $\partial_T f<0$ when the temperature suppresses the vertical transport. Since the thermal diffusion length ℓ_T is typically much larger than the device thickness w, the heat dynamics in the device can be modeled by the two-dimensional equation

$$c\rho w\frac{\partial T}{\partial t}=\kappa w\Delta_\perp T+Ju-\gamma(T-T_{\rm ext}),\quad \Delta_\perp\equiv\partial_x^2+\partial_y^2. \tag{3}$$

Here T corresponds to the mean value of temperature along the device vertical direction, and c, ρ, and κ are the specific heat, density, and heat conductivity of the semiconductor material, respectively. The second and third terms on the right-hand side of Eq. (3) describe Joule heating and cooling due to contact with the environment, respectively. $T_{\rm ext}$ is the temperature of the external cooling reservoir. For multilayer structures with classical transport, $T_{\rm ext}$ is usually room temperature. The coefficient γ is a heat transfer coefficient (per unit square of the structure) that characterizes the efficiency of external cooling. The characteristic relaxation time τ_T, diffusion length ℓ_T, and propagation velocity v_T are given by

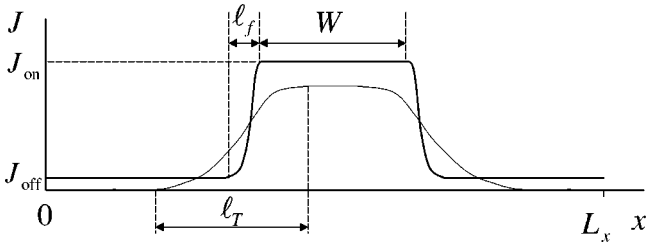

FIG. 2. Current density profile in a filament (thick line). The thin line denotes the temperature profile in the static filament.

$$\tau_T\equiv\frac{c\rho w}{\gamma},\quad \ell_T\equiv\sqrt{\frac{\kappa w}{\gamma}},\quad v_T\equiv\frac{\ell_T}{\tau_T}=\sqrt{\frac{\kappa\gamma}{c^2\rho^2 w}}. \tag{4}$$

The modified model that include temperature is given by the following set of equations:

$$\frac{\partial a}{\partial t}=\nabla_\perp(D_a(a)\nabla_\perp a)+f(a,u,T), \tag{5}$$

$$\tau_T\frac{\partial T}{\partial t}=\ell_T^2\Delta_\perp T+(Ju/\gamma+T_{\rm ext}-T), \tag{6}$$

$$\tau_u\frac{du}{dt}=U_0-u-R\int_S J(a,u,T)dxdy. \tag{7}$$

The variable T plays a role of a second inhibitor.

In the following we assume that the device is elongated along the x direction ($L_x\gg L_y$)and take only this lateral dimension into account. We also neglect the direct effect of temperature on the current density J in Eq. (7).

III. CURRENT FILAMENT AND MECHANISM OF ITS MOTION

A current density filament in a long structure represents a domain of the high current density state embedded into a low current density state (Fig. 2). The width of the filament wall ℓ_f is of the order of $\ell_f\sim\sqrt{D_a/\partial_a f}$.[7] For $T=T_{\rm ext}$ the voltage $u_{\rm co}$ over the device with a steady filament is chosen by the condition known as the "equal area rule"[2,5]

$$\int_{a_{\rm off}}^{a_{\rm on}} f(a,u_{\rm co},T=T_{\rm ext})D_a(a)da=0, \tag{8}$$

which ensures that production and annihilation of the inhibitor a in the filament wall compensate each other. When the integral in Eq. (8) is positive or negative, the balance is bro-

ken, and the filament walls move in such a way that the high current density state or the low current density state, respectively, expand. Since $\partial_u f>0$, the filament expands for $u>u_{co}$ and shrinks for $u<u_{co}$. The filament has neutral stability with respect to the lateral shift when T is kept constant.[8]

The current-voltage characteristic of the filament in a long structure is practically vertical,[2,5,8,41] and bends in the upper and lower parts when the filament becomes narrow (Fig. 1). The bent parts correspond to current density intervals $[J_{off};J_{off}+(\ell_f/L_x)J_{on}]$ and $[J_{on}-(\ell_f/L_x)J_{on};J_{on}]$, where J_{on} and J_{off} are current densities in the high current density state and the low current density state, respectively. These intervals are negligible for $L_x \gg \ell_f$.[2,8,41]

The current filament is stable for sufficiently large load resistance R and small relaxation time τ_u.[10,8] We assume that $\tau_u \ll \tau_a, \tau_T$, and hence Eq. (7) essentially represents a constraint imposed on the dynamics determined by Eqs. (5) and (6). Without loss of generality we can also assume that the regime of the external circuit is close to the current-controlled regime: $U_0 \gg u_{co}$ and the total current $I \approx U_0/R$ is constant. The width of the filament is directly proportional to the total current I,

$$W=\frac{1}{L_y}\frac{I-L_xL_y\cdot J_{off}}{J_{on}-J_{off}}\approx\frac{1}{L_y}\frac{I}{J_{on}}, \tag{9}$$

where the last equality takes into account that typically $J_{on} \gg J_{off}$.

Qualitatively, the mechanism of filament motion in the presence of self-heating is the following. With an increase of temperature the stationary balance (8) within the filament wall is broken due to the temperature dependence of the local kinetic function $f(a,u,T)$. As long as the temperature profile $T(x)$ is symmetric, the left and right walls of the filament are equal and the filament would either expand or shrink. This is forbidden since the total current is conserved by the global constraint (7). An increase of temperature is compensated by the deviation of u from u_{co} in such a way that the stationary balance within the filament wall is restored. Since $\partial_u f>0$ and $\partial_T f<0$, the voltage increases, but the filament stays steady. In contrast, for antisymmetric temperature fluctuations the balance is disturbed differently in the left and right filament walls, becoming positive on one side and negative on the other side. Potentially, this spontaneous instability leads to the motion of a filament as a whole preserving the total current. In the traveling filament the temperature at the back edge exceeds the temperature at the leading edge due to the heat inertia of the semiconductor structure. Hence the filament motion becomes self-sustained. Below we present an analytical theory of this effect. The theory is based on the following assumptions.

(i) The effect of self-heating is small and can be considered as a perturbation; hence the local kinetic function can be linearized near $T=T_{ext}$ and $u=u_{co}$ as

$$f(a,u,T)=f(a,u_{co},T=T_{ext})+(u-u_{co})\partial_u f+(T-T_{ext})\partial_T f. \tag{10}$$

(ii) The transverse dimension of the semiconductor structure is large in the sense that $L_x \gg \ell_f, \ell_T$; therefore only wide filaments with $W \gg \ell_f$ are relevant and the effect of boundaries is negligible.

(iii) The width of the filament wall ℓ_f is much smaller than the thermal diffusion length ℓ_T, and therefore the temperature variation within the filament walls can be neglected.

IV. STATIONARY MOTION OF A FILAMENT: GENERAL PROPERTIES

A. Model equations in the comoving frame

For stationary motion of a filament with a constant velocity v the solution of Eqs. (5), (7), and (6) has the form

$$a(x,t)=a(x-vt),T(x,t)=T(x-vt),\quad u=\text{const.} \tag{11}$$

In the comoving frame $\xi=x-vt$, Eqs. (5), (7), and (6) are

$$[D_a(a)a']'+va'+f(a,u,T)=0, \tag{12}$$

$$\ell_T^2T''+v\tau_TT'+(Ju/\gamma+T_{ext}-T)=0, \tag{13}$$

$$U_0-u-RL_y\langle J(a,u)\rangle=0. \tag{14}$$

Here the prime $(\cdots)'$ denotes the derivative with respect to ξ and angular brackets $\langle\cdots\rangle$ denote an integration over ξ. For the sufficiently large L_x the boundary conditions are given by

$$a(\xi)\to a_{off}(u),T(\xi)\to T_\star \quad \text{for} \quad \xi\to\pm\infty, \tag{15}$$

where

$$T_\star\equiv T_{ext}+J_{off}(u_{co})u_{co}/\gamma \tag{16}$$

is the steady state temperature corresponding to the low current density state.

B. Filament velocity and voltage over the structure

In order to calculate the velocity of the filament and the voltage on the structure with traveling filament, we note that for given u and T both filament walls can be treated as propagating fronts in a bistable medium and use the standard formula[25,31,41]

$$v=\frac{2\int_{a_{off}}^{a_{on}}f(a,u,T)D_a(a)da}{\langle D_a(a)(a_0')^2\rangle}, \tag{17}$$

where the filament profile is approximated by the steady state profile $a_0(x)$. Equation (17) implies that the velocity v is proportional to the disbalance of production and annihilation of the activator a in the filament wall. Here T is the temperature within the filament wall under consideration, which is taken as constant according to the assumption $\ell_f \ll \ell_T$. The factor 2 in the numerator appears because a_0 corresponds to the pattern that consists of two fronts. Positive and nega-

tive velocities correspond to the propagation of the high current density state into the low current density state and vice versa, respectively.

Linearizing the local kinetic function according to Eq. (10) and taking into account Eq. (8), we obtain

$$v(u,T)=\frac{2}{\langle D_a(a)(a_0')^2\rangle}\times\int_{a_{\rm off}}^{a_{\rm on}}[(u-u_{\rm co})\ \partial_u f+(T-T_{\rm ext})\partial_T f]D_a(a)da. \tag{18}$$

Hereafter, all derivatives are taken at $u=u_{\rm co}$ and $T=T_{\rm ext}$.

Equation (18) should be applied separately to the left and the right filament walls. In terms of Eq. (18) the respective velocities have the same absolute value but different signs

$$v(u,T_R)=-v(u,T_L), \tag{19}$$

where T_R and T_L are temperatures at the right and left walls, respectively. Equations (18) and (19) together yield

$$v=\frac{T_R-T_L}{\langle D_a(a)(a_0')^2\rangle}\int_{a_{\rm off}}^{a_{\rm on}}\partial_T f D_a(a)da, \tag{20}$$

$$u=u_{\rm co}+B\left(\frac{T_L+T_R}{2}-T_{\rm ext}\right), \tag{21}$$

$$B\equiv-\frac{\int_{a_{\rm off}}^{a_{\rm on}}\partial_T f D_a(a)da}{\int_{a_{\rm off}}^{a_{\rm on}}\partial_u f D_a(a)da}.$$

According to Eqs. (20) and (21) the filament velocity is proportional to the difference of temperatures at the filament edges (T_L-T_R), while the voltage deviation from $u_{\rm co}$ is proportional to the mean value $(T_L+T_R)/2$. For $\partial_T f<0$ the coefficient B is positive, and hence the voltage increases with an increase of temperature. The filament moves to the right $(v>0)$when $T_L>T_R$ and to the left $(v<0)$when $T_L<T_R$.

It is worth mentioning that Eq. (20) derived for the wide filament with narrow walls is a special case of the general expression

$$v=-\frac{\langle\partial_T f D_a(a)T(\xi)a_0'\rangle}{\langle D_a(a)(a_0')^2\rangle}, \tag{22}$$

which is applicable for any filament shape and temperature profile $T(\xi)$ satisfying boundary condition (15). Similar to Eq. (17), Eq. (22) can be obtained by multiplying Eq. (12) by $D_a(a)a'$, integrating over ξ and using expansion (10).

Equations (20),(21) do not refer exclusively to the case of Joule self-heating. They are applicable regardless of the origin of the inhomogeneous temperature profile in the semiconductor structure. We conclude that when temperature suppresses the vertical transport $(\partial_T f<0)$, as happens in the case of an impact ionization mechanism of S-type characteristic, the filament generally moves against the temperature gradient. In the case when the influence of heating is positive $(\partial_T f>0)$, as happens, for example, when the thermogeneration mechanism is involved, the filament moves along the temperature gradient. Note that a similar formula for the filament velocity in magnetic field was derived in Ref. 43. In both cases the velocity is proportional to the coupling between the neutral translation mode of the steady filament $\Psi_T\sim a_0'$ (the so-called Goldstone mode) and the profile of the externally applied field.

C. Temperature profile in the moving filament

For a filament with narrow walls $(\ell_f\ll\ell_T)$the heat equation (13) is piecewise linear and the temperature profile $T(\xi)$ can be found analytically (see the Appendix). Consequently, the temperatures T_L and T_R can be presented explicitly as functions of the filament velocity v and width W. It is convenient to introduce the normalized difference and the sum of T_L and T_R:

$$\Delta_{LR}\equiv\frac{T_L-T_R}{T^\star-T_\star},\quad \Sigma_{LR}\equiv\frac{T_L+T_R-2T_\star}{T^\star-T_\star}, \tag{23}$$

where the temperatures $T^\star$ and $T_\star$ are stationary uniform solutions of the heat equation (6) corresponding to uniform on and off states, respectively[44]:

$$T^\star=T_{\rm ext}+J_{\rm on}(u_{\rm co})u_{\rm co}/\gamma, \tag{24}$$

and $T_\star$ is defined by Eq. (16). Typically $T_\star\approx T_{\rm ext}$.

From solution (A2) of the heat equation we obtain

$$\Delta_{LR}=\frac{1}{\sqrt{1+\tilde v^2}}\{\tilde v-\exp(-\tilde W\sqrt{1+\tilde v^2})\times[\tilde v\cosh(\tilde W\tilde v)+\sqrt{1+\tilde v^2}\sinh(\tilde W\tilde v)]\}, \tag{25}$$

$$\Sigma_{LR}=1-\frac{1}{\sqrt{1+\tilde v^2}}\exp(-\tilde W\sqrt{1+\tilde v^2})\times[\tilde v\sinh(\tilde W\tilde v)+\sqrt{1+\tilde v^2}\cosh(\tilde W\tilde v)], \tag{26}$$

where

$$\tilde v=\frac{v}{2v_T},\quad \tilde W=\frac{W}{\ell_T}.$$

The dependencies $\Delta_{LR}(v,W)$ and $\Sigma_{LR}(v,W)$ are shown in Fig. 3. The temperature difference is equal to zero for $v=0$, when the temperature profile is symmetric, and reaches a maximum at a certain value of v [Fig. 3(a)]. The temperature difference decreases with further increase of v and vanishes for large velocities $(v\gg W/\tau_T)$when the filament moves too fast to heat the semiconductor structure. The average temperature and, according to Eq. (21), the voltage u monotonically decrease as v increases [Fig. 3(b)]. Hence the onset

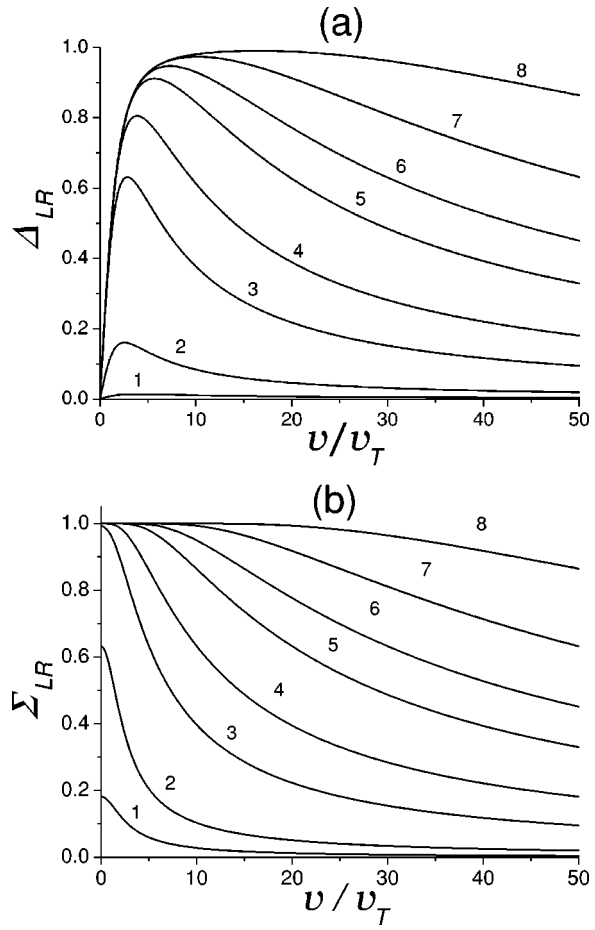

FIG. 3. The normalized difference Δ_{LR} (a) and the sum Σ_{LR} (b) of the temperatures in the filament walls T_L and T_R as functions of the filament velocity v for different filament widths W. Δ_{LR} and Σ_{LR} are defined by Eqs. (23), (25), and (26). Curves 1–8 correspond to $W/\ell_T = 0.2,1,5,10,20,30,50,$ and 100, respectively.

of filament motion is always accompanied by a certain voltage drop. Both $(T_L - T_R)$ and $(T_L + T_R)$ increase with filament width W for a given v.

V. SELF-CONSISTENT DETERMINATION OF FILAMENT VELOCITY

In the regime of Joule self-heating, the stationary filament motion with a certain velocity occurs when the moving filament generates the temperature profile with the temperature difference $(T_L - T_R)$ which is exactly needed to support this motion. Combining Eqs. (20), (23), and (25), we obtain a transcendental equation for the filament velocity v:

$$\frac{v}{v_0} = \Delta_{LR}(v,W), \tag{27}$$

$$v_0 \equiv -\frac{T^\star - T_\star}{\langle D_a(a)(a_0')^2\rangle}\int_{a_{\rm off}}^{a_{\rm on}} \partial_T f D_a(a)\,da. \tag{28}$$

Here v_0 is the upper limit of the filament velocity which is achieved for $T_L - T_R = T^\star - T_\star$. This velocity characterizes the effect of temperature on the filament dynamics. The function Δ_{LR} is explicitly given by Eq. (25). Δ_{LR} is odd with respect to v, reflecting the symmetry between left and right directions of the filament motion. Hence nontrivial solutions $v^\star \neq 0$ of Eq. (27) always come in pairs $(v^\star, -v^\star)$. Having this in mind, below we discuss only non-negative solutions $v \geqslant 0$. Note that $v_0 < 0$ for $\partial_T f > 0$ (positive influence of temperature on vertical transport), and therefore Eq. (28) has only the trivial solution $v = 0$: filament motion is not possible. We shall focus on the case $\partial_T f < 0$ when $v_0 > 0$.

It is immediately evident from Fig. 3(a) that Eq. (27) has either one or two non-negative roots depending on v_0 and W. Solution $v^\star = 0$, corresponding to a steady filament, exists for all parameter values. A nontrivial solution $v^\star > 0$, that corresponds to the traveling filament, exists if

$$v_0 \left.\frac{d\Delta_{LR}}{dv}\right|_{v=0} > 1. \tag{29}$$

This condition follows from simple geometrical consideration and means that at $v = 0$ the slope of the $\Delta_{L,R}(v,W)$ dependence, which corresponds to the right-hand side of Eq. (28), is larger than the slope of the straight line v/v_0, which corresponds to the left-hand side of the same equation. Hence Eq. (28) has a nontrivial solution [see Fig. 3(a)]. Physically, Eq. (29) means that the temperature difference $(T_L - T_R)$ increases sufficiently fast with filament velocity v. As we show below, this makes a steady solution $v = 0$ unstable and results in a self-sustained filament motion.

When the root $v = 0$ is unique, the corresponding stationary filament is stable because $\Delta_{LR}(v) < v/v_0$ for $v > 0$. This inequality means that a traveling filament generates a temperature difference $(T_L - T_R)$ which is not sufficient to support its motion. The situation changes when condition (29) is met: in this case $\Delta_{LR}(v) > v/v_0$ for $v > 0$, and the steady solution is unstable. It means that the steady filament loses stability simultaneously with the appearance of a nontrivial solution $v^\star > 0$ which corresponds to a traveling filament. Hence, Eq. (29) represents a condition for the spontaneous onset of filament motion. We discuss the bifurcation from static to traveling filament in more detail in Sec. VI.

A traveling filament is stable because $\Delta_{LR}(v) > v/v_0$ for $v < v^\star$ and $\Delta_{LR}(v) < v/v_0$ for $v > v^\star$. Indeed, these inequalities mean that if v decreases the temperature difference $(T_L - T_R)$ increases and hence, according to Eq. (20), the filament velocity should increase again. In the same way, with an increase of v the difference $(T_L - T_R)$ decreases and therefore the filament slows down.

In Fig. 4(a) we present the numerical solutions $v(W)$ of Eq. (27) for different values of the parameter v_0. For a given v_0 the motion is possible for filaments whose width exceeds a certain threshold $W_{\rm th}(v_0)$ (Fig. 5). With increasing W the filament velocity increases and eventually saturates. We discuss the analytical approximations of the front velocity in Secs. VII and VIII.

In Fig. 4(b) we present the voltage u in the regime of

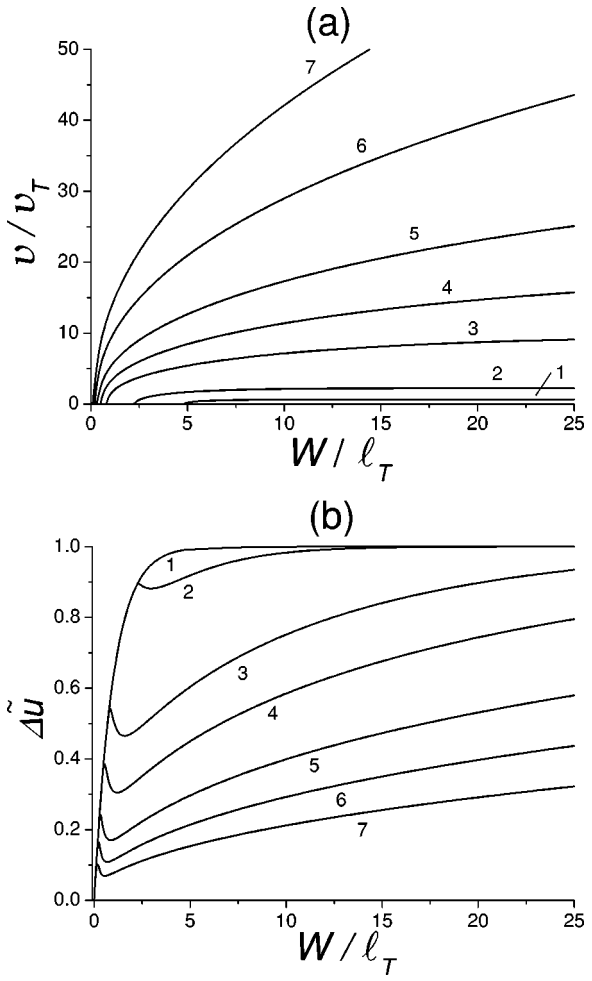

FIG. 4. The filament velocity v (a) and normalized voltage on the structure $\Delta\tilde{u}$ (b) as functions of the filament width W for different values of the parameter v_0. $\Delta\tilde{u}$ is defined by Eq. (30). Curves 1–7 correspond to $v_0=2.1$, 3, 10, 20, 50, 100, and 200, respectively. Peaks on the voltage curves are related to the onset of the filament motion.

current filamentation obtained by substituting numerical solutions of Eq. (27) into Eqs. (21) and (26). The normalized deviation of u from u_{co},

$$\Delta\tilde{u}=2\ \frac{B^{-1}(u-u_{\mathrm{co}})-(T_\star-T_{\mathrm{ext}})}{T^\star-T_\star} \tag{30}$$

is shown, where B is determined by Eq. (21). The voltage drop, clearly visible on curves 2–7, is associated with the onset of filament motion. With further increase of W the voltage increases again. Curve 1 is calculated for $v_0/v_T=2.1$, which is close to the threshold value $v_0/v_T=2$, and practically coincides with the curve for a static filament. Since the filament width W is directly proportional to the total current I [see Eq. (9)], Fig. 4(b) actually represents the current-voltage characteristic of the structure with a traveling filament. In particular, the voltage drop associated with the onset of filament motion can be observed experimentally when a filament starts to travel due to increase of the total current I.

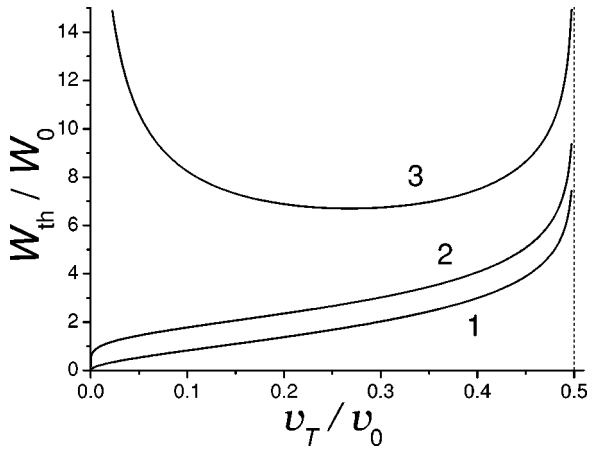

FIG. 5. Normalized threshold filament width W_{th} corresponding to the onset of the filament motion as a function of v_T/v_0. Curve 1 shows W_{th} normalized to the thermal diffusion length: $W_0=\ell_T$. Curve 2 shows W_{th} normalized to the quantity $W_0=(D_T^2\tau_T/v_0)^{1/3}$, which does not depend on the heat transfer coefficient γ. Curve 3 shows W_{th} normalized to the quantity $W_0=\sqrt{D_T/v_0}$, which does not depend on the structure thickness w.

VI. ONSET OF THE FILAMENT MOTION

To analyze the onset of filament motion and propagation of slow filaments we expand Δ_{LR} with respect to v/v_T up to second order:

$$\Delta_{LR}(v,W)\approx\frac{v}{2v_T}\left[1-\frac{1}{8}\left(\frac{v}{v_T}\right)^2\right]A(W),$$
$$A(W)\equiv\left[1-\left(1+\frac{W}{\ell_T}\right)\ \exp\left(-\frac{W}{\ell_T}\right)\right]. \tag{31}$$

In this case the temperature profile is close to the symmetric stationary profile given by Eq. (A4).

Substituting Eq. (31) into Eq. (29), we obtain an explicit condition for the onset of filament motion

$$\frac{v_0}{2v_T}A(W)>1. \tag{32}$$

This condition can be further simplified for narrow and wide filaments:

$$\frac{v_0}{4v_T}\left(\frac{W}{\ell_T}\right)^2>1 \quad \text{for} \quad W\ll\ell_T, \tag{33}$$

$$\frac{v_0}{2ev_T}\left(\frac{W}{\ell_T}+e-3\right)>1 \quad \text{for} \quad W\sim\ell_T, \tag{34}$$

$$\frac{v_0}{2v_T}>1 \quad \text{for} \quad W\gg\ell_T, \tag{35}$$

where e is the natural logarithmic base. Since $A(W)<1$, it follows from Eq. (32) that regardless to the filament width W the filament motion is not possible if $v_0<2v_T$. If $v_0>2v_T$, the filaments whose width W overcomes the threshold $W_{\rm th}$ determined by Eq. (32) start to move, whereas smaller filaments remain steady. The dependence of $W_{\rm th}$ on v_0/v_T is shown in Fig. 5, curve 1. This dependence can be approximated as

$$W_{\rm th}\approx 2\ell_T\sqrt{\frac{v_T}{v_0}} \quad \text{for} \quad W_{\rm th}\ll\ell_T, \tag{36}$$

$$W_{\rm th}\approx \ell_T\left(2e\frac{v_T}{v_0}+3-e\right) \quad \text{for} \quad W_{\rm th}\sim\ell_T, \tag{37}$$

$$W_{\rm th}\approx -\ell_T\ln\left(1-\frac{2v_T}{v_0}\right) \quad \text{for} \quad W_{\rm th}\gg\ell_T. \tag{38}$$

The bifurcation to a traveling filament resembles a supercritical pitchfork bifurcation:[45] at the bifurcation point $W=W_{\rm th}$ the static solution becomes unstable, and simultaneously two stable branches corresponding to the filaments traveling to the left and to the right appear [Fig. 4(a)]. This bifurcation can be understood in terms of a stability analysis of the current filament performed in Ref. 8 for the standard two-component model (1),(2): The spectrum of eigenmodes of a static filament includes a neutral mode Ψ_T with zero eigenvalue $\lambda_T=0$ which corresponds to translation. Existence of this neutral mode reflects the translation invariance of a static filament on a large spatial domain. In the extended model (5), (6), (7) the bifurcation to a traveling filament is characterized by symmetry breaking when λ_T becomes positive. This becomes possible due to the coupling between the master equation (5) and the heat equation (6) when $\partial_T f<0$. Note that for $\partial_T f>0$ the eigenvalue of the translation mode λ_T becomes negative. This corresponds to self-pinning of the filament.

VII. PROPAGATION OF SLOW FILAMENTS

Substituting Eq. (31) into Eq. (27) we obtain an explicit equation for the filament velocity which is applicable for slow filaments:

$$v(W)=2v_T\sqrt{\frac{v_0}{v_T}A(W)-2}, \tag{39}$$

where $A(W)$ is defined in Eq. (31). The asymptotic value is given by

$$v\to 2v_T\sqrt{\frac{v_0}{v_T}-2} \quad \text{for} \quad \frac{W}{\ell_T}\to\infty. \tag{40}$$

Equation (39) approximates $v(W)$ with an accuracy of 10% up to the parameter value $v_0/v_T=3$ [curve 2 on Fig. 4(a)], despite the fact that it is derived for $v\ll v_T$. This wide range of applicability is due to the particulary smooth behavior of $\Delta_{LR}(v)$ to the left of its peak value [see Fig. 3(a)].

VIII. PROPAGATION OF FAST FILAMENTS

In the limit $v\gg v_T$ the temperature profile is strongly asymmetric [see Eq. (A5)], and the temperature at the leading edge is close to $T_\star$. Equation (25) can be expanded with respect to v_T/v :

$$\Delta_{LR}(v,W)=1-\exp\left(-\frac{W}{v\tau_T}\right)-\left(\frac{v_T}{v}\right)^2\left[2-\exp\left(-\frac{W}{v\tau_T}\right)\right]. \tag{41}$$

According to Eq. (A3) the characteristic scale of the temperature profile for the fast filament is determined by $(\lambda^+)^{-1}\approx v\tau_T$ which exceeds ℓ_T. To keep the diffusion correction, we expand up to second order.

Analytical results are available for the case of a narrow filament ($W\ll v\tau_T$) and a wide filament ($W\gg v\tau_T$). In the first case ($W\ll v\tau_T$) the temperature inside the filament increases linearly, and T_L is much smaller than $T^\star$. For $W\ll v\tau_T$, Eq. (41) reduces to

$$\Delta_{LR}(v,W)\approx\frac{W}{\ell_T}\left(\frac{v_T}{v}\right)-\left(\frac{v_T}{v}\right)^2. \tag{42}$$

Substituting Eq. (42) into Eq. (27) we obtain the filament velocity

$$v(W)\approx\sqrt{\frac{Wv_0}{\tau_T}}-\frac{\ell_T v_T}{2W} \quad \text{for} \quad W\ll v\tau_T. \tag{43}$$

Note that in Eq. (43) the leading term does not depend on the heat diffusion.

In the case of a wide filament ($W\gg v\tau_T$) the temperature at the back edge is close to the maximum value $T^\star$. The front velocity is approximated by

$$v(W)\approx v_0-\frac{2v_T^2}{v_0}-\exp\left(-\frac{W}{v_0\tau_T}\right)\left[v_0-\frac{2v_T^2}{v_0}\right] \quad \text{for} \quad W\gg v\tau_T \tag{44}$$

and saturates at

$$v\to v_0-\frac{2v_T^2}{v_0} \quad \text{for} \quad \frac{W}{v_0\tau_T}\to\infty.$$

IX. DISCUSSION

A. Scales hierarchy — which limiting case is relevant?

The thermal relaxation time τ_T of the semiconductor structure can be straightforwardly determined by experiment. Therefore it is convenient to use it as basic parameter and to express ℓ_T and v_T via τ_T. Depending on the structure thickness and design, the effective value of τ_T varies from 100–200 ns for transistorlike structures of electrostatic discharge protections devices[39] (the structure thickness $w\sim 10$ μm) to $\sim 10-100$ ms for power devices (the structure thickness $w\sim 100-500$ μm).[40] It follows from Eq. (4) that parameters ℓ_T and v_T are related to τ_T via

$$\ell_T = \sqrt{D_T \tau_T}, \quad v_T = \sqrt{\frac{D_T}{\tau_T}}, \quad D_T \equiv \frac{\kappa}{c\rho}, \tag{45}$$

where the thermal diffusivity D_T depends only on material parameters. We take $D_T = 0.92$ and $0.25\ \mathrm{cm}^2/\mathrm{s}$ for Si and GaAs, respectively. Consequently, ℓ_T and v_T are of the order of 10 μm and 10^3 cm/s, respectively, for small devices ($\tau_T \sim 100$ ns, $w \sim 10$ μm). We obtain 1 mm and 10 cm/s, respectively, for large power devices ($\tau_T \sim 10$ ms, $w \sim 100$ μm). Hence in most devices the filament width W is of the order of the thermal diffusion length ℓ_T or smaller, and ℓ_T is smaller but comparable to the transverse dimension of the structure L. In particular, it implies that in the regime of self-heating the maximum temperature in the current filament is much smaller than $T^\star$. For $W \lesssim \ell_f$ and sufficiently far from the bifurcation point $v_0 = 2v_T$ the filament velocity is well described by formula (43), where the second term can be neglected.

B. Stimulating the filament motion

The motion of the filament delocalizes the heating of semiconductor structure and thus is desirable in applications. Generally, the start of the filament motion becomes easier with increasing v_0 and decreasing v_T and ℓ_T [see Eq. (32) and Fig. 5, curve 1]. However, these parameters cannot be varied independently. Below we focus on the effect of the structure parameters which enter our model: the heat transfer coefficient γ and the structure thickness w.

Curve 2 in Fig. 5 shows the threshold filament width W_{th} normalized by the quantity $(D_T^2 \tau_T / v_0)^{1/3}$ which does not depend on the heat transfer coefficient γ. Taking into account that $v_T / v_0 \sim \gamma^{3/2}$, we conclude that a decrease of γ makes the onset of the filament motion easier. This occurs due to the increase of v_0 which, according to Eqs. (16), (24), and (28), scales as $v_0 \sim \gamma^{-1}$. However, an easy start of the filament motion in structures with inefficient cooling comes at the price of increasing the temperature in the filament, which makes static filaments more dangerous.

Curve 3 in Fig. 5 shows W_{th} normalized by the quantity $(D_T / v_0)^{1/2}$ which does not depend on the structure thickness w. Since $v_T / v_0 \sim w^{-1/2}$, we see that the dependence of W_{th} on w is nonmonotonic. The physically relevant situation $W \lesssim \ell_T$ corresponds to the left part of curve 3 where W_{th} increases with w. The effect is due to an increase of $\ell_T \sim w^{1/2}$. Thus, for a fixed value of v_0, thinner structures are preferable for the filament motion.

For efficient delocalization of heating in a realistic structure it is important that the filament is not pinned when it approaches the device edge, but reflects and continues traveling in the opposite direction. Such a reflection from the device edge is indeed possible and has been observed in experiments.[23,27,39] The interaction of the thermally driven traveling filament with boundaries is beyond the scope of this paper and will be considered elsewhere.

C. Transient behavior

A static current filament typically appears due to the spatial instability of the uniform state on the middle branch of the current-voltage characteristic (see Fig. 1). This occurs[7] on the time scale τ_a, which is typically smaller than the thermal time scale τ_T. First the voltage settles at $u = u_{\mathrm{co}}$, and only then the temperature starts to increase. According to Eq. (21) the Joule heating is accompanied by an increase of u. As soon as the static filament gets hot, the bifurcation to the traveling filament occurs, provided that condition (29) is satisfied. The onset of filament motion leads to a certain voltage drop, though u remains larger than u_{co} [see Eq. (21) and Fig. 4(b)]. The motion can start before the steady temperature profile in the static filament is established, but the nonmonotonic dynamics of u remain qualitatively the same.

D. Self-motion and self-pinning

As pointed out in Sec. VI, we predict, instead of self-motion, a self-pinning of the filament at its initial location due to the Joule self-heating in the case $\partial_T f > 0$. For example, it happens when the temperature becomes high enough for thermogeneration to set in. This typically precedes thermal destruction of the semiconductor structure due to local overheating. Equation (20) also suggests an experimental method to distinguish between a positive ($\partial_T f > 0$) and negative ($\partial_T f < 0$) influence of temperature on vertical transport by observing the filament dynamics in an externally applied temperature gradient: filaments move along or against the temperature gradient for $\partial_T f > 0$ or $\partial_T f < 0$, respectively.

E. Motion of low-current filaments

S-shaped current-voltage characteristics exhibit a formal duality between high and low current density branches. Therefore, apart from high-current filaments, there are patterns in form of low-current filaments: domains of low current density embedded into an on state.[5,8] Such filaments correspond to the upper part of the filamentary current-voltage characteristic (Fig. 1), where the average current density is close to J_{on}. In the case $\partial_T f < 0$ low-current filaments also undergo a bifurcation from static to traveling filaments. Expressions (20) and (21) remain valid as they are, whereas in Eqs. (25) and (26) $T^\star$ and $T_\star$ should be exchanged. The onset of motion results in an increase, rather than a decrease, of the voltage in this case. The duality between on and off states is broken when vertical transport is suppressed near the structure boundary due to a certain process at the lateral edge of the semiconductor structure, e.g., surface recombination or surface leak in the p-n junction. (This effect can be modeled by Dirichlet boundary conditions $a = 0$ imposed on the variable a at $x = 0, L_x$.[5]) In this case the effect of boundaries can not be neglected for average current densities close to J_{on} even in the limit $L_x \gg \ell_f$. The current-voltage characteristic, instead of showing hysteresis, exhibits a continuous crossover from the filamentary branch to the branch of quasiuniform high current density states at high current.[5] Then, only high-current filaments are observable.

F. Reaction-diffusion models for traveling spots

The model (5), (6), (7) belongs to the same class of three-component reaction-diffusion models as models for traveling spots in active media discussed in Refs. 46–51. In contrast to the common two-component activator-inhibitor model,[22,31] three-component models are capable of describing localized traveling patterns not only on a one-dimensional spatial domain, but also on spatial domains of higher dimensions.[46,47] The transition from static to traveling spots takes place with an increase of the relaxation time of the first inhibitor,[46] in the same way as it occurs in the common two-component model of pulse propagation in excitable media.[31] The second fast long-range inhibitor plays an essential role only in the two- or three-dimensional case: it prevents a lateral spreading of the traveling spot which otherwise destroys the spatially localized solution and eventually leads to the development of a spiral wave.[46,47]

This additional inhibition can be either global[46] or local.[47] In the first case, the inhibitor has the same value in the whole system. This value depends on the mean value of other dynamical variables in the system and is governed by an integrodifferential equation. This corresponds to the global coupling of a spatially extended nonlinear system. In the second case, the additional inhibitor is governed by a conventional reaction-diffusion equation. For traveling spots, the difference between these two cases becomes crucial only when several spots are considered on a two- or higher-dimensional domain: the system of several spots is unstable when the additional inhibition is global, but becomes stable when it is local.[47] This difference vanishes when only one spot is present, or the spatial domain is one dimensional.[47] Global coupling through the gas phase occurs in the surface reactions[52–55] and can be implemented as a global feedback loop in the light-sensitive Belousov-Zabotinsky reaction.[56,57] Implementation of the respective control loop has allowed the observation of localized traveling patterns in these systems.[55,57]

In contrast to the three-component models discussed in Refs. 46 and 47, in the model (5), (6), (7) both inhibitors are needed for the onset of filament motion already in the one-dimensional case. Consequently, the bifurcation to a traveling filament is also different. This reflects the fact that we start with a static pattern in a bistable medium with fast global inhibition (voltage u). This global inhibition is due to the external circuit and represents an inherent feature of the spatiotemporal dynamics of a bistable semiconductor: for any evolution of the current density pattern which is accompanied by the variation of the total current, the voltage at an external series resistance changes, causing the variation of the voltage across the device. This inhibition is crucial for the existence of current filaments which become unstable when the global coupling is eliminated by operating the device in the voltage-controlled regime.[2,8,10] The motion of the filament is induced by the effect of another slow diffusive inhibitor (temperature T). A similar nonlinear mechanism causes the motion of current filaments obtained by numerical simulations in Refs. 23 and 48. However, Refs. 23 and 48 focus on a specific type of multilayer thyristorlike structures. The model of these devices[27] assumes that the second inhibitor is a certain internal voltage, not a temperature.

It is worth mentioning, that self-heating may also trigger temporal relaxation-type oscillations of a current-density filament. This effect has been observed in a reversely biased p-i-n diode and is explained by a similar three-component reaction-diffusion model.[58]

X. SUMMARY

Joule self-heating of a current density filament in a bistable semiconductor structure might result in the onset of lateral motion. This occurs when an increase of temperature has a negative impact on the vertical (cathode-anode) transport. Such negative feedback takes place when bistability of semiconductor structures is related to avalanche impact ionization, because the impact ionization rate decreases with temperature at high electrical fields.[4] Examples of such devices are avalanche transistors,[18] reversely biased p-i-n diodes in the regime of avalanche injection, electrostatic discharge protection devices operated in the avalanche regime,[28] and multilayer thyristorlike structures.[21,27] Traveling filaments can be consistently described by generic nonlinear model (5), (6), (7).

Generally, filaments move against the temperature gradient with a velocity proportional to the temperature difference at the filament edges [Eq. (20)]. In the regime of Joule self-heating, the strength of coupling between the master equation (5), which controls the current density dynamics, and the heat equation (6) can be characterized by a single parameter v_0 [Eq. (28)], which has a dimension of velocity. The filament velocity v is determined by the transcendental equation (27). The condition for the spontaneous onset of filament motion (29) depends on the ratio of v_0 and the thermal velocity v_T, and on the ratio of the filament width W and the thermal diffusion length ℓ_f. Filament motion is never possible for $v_0 < 2v_T$. For $v_0 > 2v_T$, static filaments whose width W exceeds a certain threshold W_{th} [Eq. (32), curve 1 in Fig. 5] become unstable and start to travel. The filament velocity v and the voltage on the structure u are shown in Fig. 4. For most semiconductor structures $W \lesssim \ell_T$, and sufficiently far from the bifurcation point $v_0 = 2v_T$ the filament velocity can be approximated by a truncated version of Eq. (43):

$$v \approx \sqrt{\frac{W v_0}{\tau_T}}.$$

Heating of the static filament is accompanied by an increase of the voltage u [Eq. (21)]. With the onset of filament motion the voltage drops, but remains higher than the voltage u_{co} [Fig. 4(b)].

Our analytical theory does not cover narrow filaments, when the flat top of the current density profile does not exist or the filament width W is comparable to the width of the filament wall ℓ_f, as well as cylindrical filaments which appear when the lateral dimensions of the semiconductor structure L_x and L_y are comparable. However, the bifurcation from static to traveling filaments and the mechanism of fila-

ment motion remain qualitatively the same in these cases. The main predictions of this theory—the increase of the filament velocity with current, the exsitence of the critical current which is needed for the filament motion, and the voltage drop associated with the onset of filament motion—can be verified experimentally.

ACKNOWLEDGMENTS

Stimulating discussions with S. Bychkhin, M. Denison, and D. Pogany are gratefully acknowledged. The author thanks A. Mikhailov and V. Zykov for helpful discussions of the results. The work was supported by the Alexander von Humboldt Foundation.

APPENDIX: SOLUTIONS OF THE HEAT EQUATION

Assuming that the front walls are thin, we present Eq. (13) as (see Fig. 2)

$$\ell_T^2 T'' + v\tau_T T' + (T^\star - T) = 0 \quad \text{for} \quad -\frac{W}{2} < \xi < \frac{W}{2}, \tag{A1}$$

$$\ell_T^2 \; T'' + v\tau_T T' + (T_\star - T) = 0 \quad \text{for} \quad \xi < -\frac{W}{2} \;\text{and}\; \xi > \frac{W}{2}.$$

Here the middle of the filament is at $\xi = 0$. $T_\star$ and $T^\star$ are defined by Eqs. (16) and (24). The solution of this piecewise linear equation is given by

$$T(\xi) = T_\star - (T^\star - T_\star)\frac{2\lambda^+}{\lambda^+ - \lambda^-}\sinh\left(\frac{\lambda^- W}{2}\right) \times \exp(\lambda^- \xi) \quad \text{for} \quad \xi > \frac{W}{2},$$

$$T(\xi) = T^\star - \frac{T^\star - T_\star}{\lambda^+ - \lambda^-}\left(\lambda^+ \exp\left[\lambda^-\left(\xi + \frac{W}{2}\right)\right] - \lambda^- \exp\left[\lambda^+\left(\xi - \frac{W}{2}\right)\right]\right) \quad \text{for} \quad -\frac{W}{2} < \xi < \frac{W}{2}, \tag{A2}$$

$$T(\xi) = T_\star - (T^\star - T_\star) \times \frac{2\lambda^-}{\lambda^+ - \lambda^-}\sinh\left(\frac{\lambda^+ W}{2}\right)\exp(\lambda^+ \xi) \quad \text{for} \quad \xi < -\frac{W}{2},$$

where λ^+ and λ^- are eigenvalues of Eq. (A1):

$$\lambda^+ = \frac{1}{\ell_T}\left[\sqrt{1 + \left(\frac{v}{2v_T}\right)^2} - \frac{v}{2v_T}\right],$$

$$\lambda^- = -\frac{1}{\ell_T}\left[\sqrt{1 + \left(\frac{v}{2v_T}\right)^2} + \frac{v}{2v_T}\right]. \tag{A3}$$

Equations (A2) allow for the determination of the temperature difference $(T_L + T_R)$ and the mean temperature $(T_L + T_R)/2$ [Eqs. (23), (25), and (26)] which are needed for the self-consistent calculation of the front velocity v and the voltage u.

Steady temperature profile. For $v = 0$ we get $\lambda^+ = -\lambda^- = 1/\ell_T$ and the corresponding symmetric temperature profile is given by

$$T(\xi) = T_\star + (T^\star - T_\star)\sinh\left(\frac{W}{2\ell_T}\right)\exp\left(-\frac{\xi}{\ell_T}\right) \quad \text{for} \quad \xi > \frac{W}{2},$$

$$T(\xi) = T^\star - (T^\star - T_\star) \times \exp\left(-\frac{W}{2\ell_T}\right)\cosh\left(\frac{\xi}{\ell_T}\right) \quad \text{for} \quad -\frac{W}{2} < \xi < \frac{W}{2}, \tag{A4}$$

$$T(\xi) = T_\star + (T^\star - T_\star)\sinh\left(\frac{W}{2\ell_T}\right)\exp\left(\frac{\xi}{\ell_T}\right) \quad \text{for} \quad \xi < -\frac{W}{2}.$$

Temperature profile in the fast filament. For $v \gg v_T$ we get $\lambda^+ = (v\tau_T)^{-1}$, $\lambda^- = -\infty$. The corresponding profile is strongly asymmetric:

$$T(\xi) = T_\star \quad \text{for} \quad \xi > \frac{W}{2},$$

$$T(\xi) = T^\star - (T^\star - T_\star)\exp\left(\frac{2\xi - W}{2v\tau_T}\right) \quad \text{for} \quad -\frac{W}{2} < \xi < \frac{W}{2},$$

$$T(\xi) = T_\star + 2(T^\star - T_\star)\sinh\left(\frac{W}{2v\tau_T}\right)\exp\left(\frac{\xi}{v\tau_T}\right) \quad \text{for} \quad \xi < -\frac{W}{2}. \tag{A5}$$

*Electronic mail: rodin@physik.tu-berlin.de

[1] B. K. Ridley, Proc. Phys. Soc. London **82**, 954 (1963).

[2] A. F. Volkov and Sh. M. Kogan, Usp. Phys. Nauk **96**, 633 (1968) [Sov. Phys. Usp. **11**, 881 (1969)].

[3] V. L. Bonch-Bruevich, I. P. Zvyagin, and A. G. Mironov, *Domain Electrical Instabilities in Semiconductors* (Consultant Bureau, New York, 1975).

[4] S. M. Sze, *Physics of Semiconductor Devices* (Wiley, New York, 1981).

[5] E. Schöll, *Nonequilibrium Phase Transitions in Semiconductors* (Springer-Verlag, Berlin, 1987).

[6] M. Shaw, V. Mitin, E. Schöll, and H. Grubin, *The Physics of Instabilites in Solid State Electron Devices* (Plenum Press, New York, 1992).

[7] A. Wacker and E. Schöll, J. Appl. Phys. **78**, 7352 (1995).

[8] A. Alekseev, S. Bose, P. Rodin, and E. Schöll, Phys. Rev. E **57**, 2640 (1998).

[9] A. F. Volkov and Sh. M. Kogan, Zh. Éksp. Teor. Fiz. **52**, 1647

(1967) [Sov. Phys. JETP **25**, 1095 (1967)].
[10] F.G. Bass, V. S. Bochkov, Yu. Gurevich, Zh. Éksp. Teor. Phys. **58**, 1814 (1970) [Sov. Phys. JETP **31**, 972 (1970)].
[11] V. Novàk, C. Wimmer, and W. Prettl, Phys. Rev. B **52**, 9023 (1995).
[12] F.-J. Niedernostheide, J. Hirschinger, W. Prettl, V. Novàk, and H. Kostial, Phys. Rev. B **58**, 4454 (1998).
[13] V. Novàk, J. Hirschinger, F.-J. Niedernostheide, W. Prettl, M. Cukr, and J. Oswald, Phys. Rev. B **58**, 13099 (1998).
[14] J. Hirschinger, F.-J. Niedernostheide, W. Prettl, and V. Novàk, Phys. Rev. B **61**, 1952 (2000).
[15] G. Schwarz, C. Lehmann, and E. Schöll, Phys. Rev. B **61**, 10194 (2000).
[16] I. V. Varlamov, V. V. Osipov, and E. A. Poltoratsky, Fiz. Tekh. Poluprovodn. **3**, 1162 (1969) [Sov. Phys. Semiconductor **3**, 978 (1970)].
[17] V. V. Osipov and V.A. Kholodnov, Fiz. Techn. Poluprovodn. **4**, 1216 (1970) [Sov. Phys. Semiconductor **4**, 1033 (1971)].
[18] V. V. Osipov and V.A. Kholodnov, Mikroelectronika **2**, 529 (1973) (in Russian).
[19] D. Jäger, H. Baumann, and R. Symanczyk, Phys. Lett. A **117**, 141 (1986).
[20] A. V. Gorbatyuk and P. B. Rodin, Solid-State Electron. **35**, 1359 (1992).
[21] A. V. Gorbatyuk and F.-J. Niedernostheide, Phys. Rev. B **59**, 13157 (1999); **65**, 245318 (2002).
[22] B. S. Kerner and V. V. Osipov, *Autosolitons* (Kluwer, Dordrecht, 1994).
[23] *Nonlinear Dynamics and Pattern Formation in Semiconductors and Devices*, edited by F.-J. Niedernostheide (Spinger-Verlag, Berlin, 1995).
[24] K. Aoki, *Nonlinear Dynamics and Chaos of Semiconductors* (Institute of Physics Publishing, Bristol, 2000).
[25] E. Schöll, *Nonlinear Spatio-Temporal Dynamics and Chaos in Semiconductors* (Cambridge University Press, Cambridge, 2001).
[26] A. Wierschem, F.-J. Niedernostheide, A. Gorbatyuk, and H.-G. Purwins, Scanning **17**, 106 (1995).
[27] F.-J. Niedernostheide, B. S. Kerner, and H.-G. Purwins, Phys. Rev. B **46**, 7559 (1992).
[28] D. Pogany, S. Bychikhin, M. Litzenberger, E. Gornik, G. Groos, and M. Stecher, Appl. Phys. Lett. **81**, 2881 (2002).
[29] M. S. Cross and P. C. Hohenberg, Rev. Mod. Phys. **65**, 851 (1993).
[30] Y. Kuramoto, *Chemical Oscillation, Waves and Turbulence* (Springer-Verlag, Berlin, 1988).
[31] A. S. Mikhailov, *Foundations of Synergetics* (Springer-Verlag, Berlin, 1994).
[32] *Self-organization in Activator-Inhibitor Systems: Semiconductors, Gas Discharge, and Chemical Active Media*, edited by H. Engel, F.-J. Niedernostheide, H.-G. Purwins, and E. Schöll (Wissenshaft & Technik, Berlin,1996).
[33] *Evolution of Spontaneous Structures in Dissipative Continious Systems*, edited by F. H. Busse and S. C. Müller (Springer, Berlin, 1998).
[34] A. Wacker and E. Schöll, Z. Phys. B: Condens. Matter **93**, 431 (1994).
[35] F.-J. Niedernostheide, H. Schulze, S. Bose, A. Wacker, and E. Schöll, Phys. Rev. E **54**, 1253 (1996).
[36] S. Bose, P. Rodin, and E. Schöll, Phys. Rev. E **62**, 1778 (2000).
[37] F. Plenge, P. Rodin, E. Schöll, and K. Krischer, Phys. Rev. E **64**, 056229 (2001).
[38] K. Penner, J. Phys. (Paris), Colloq. **49**, C4797 (1988).
[39] D. Pogany, S. Bychikhin, E. Gornik, M. Denison, N. Jensen, G. Groos, and M. Stecher, *Moving Current Filaments in ESD Protection Devices and their Relation to Electrical Characteristics* (Electron Device Society and the Reliability Society of the Institute of Electrical and Electronics Engineers, Inc. 2003).
[40] G. Wachutka, IEEE Trans. Electron Devices **38**, 1516 (1991).
[41] M. Meixner, P. Rodin, E. Schöll, and A. Wacker, Eur. Phys. J. B **13**, 157 (2000).
[42] P. Rodin and E. Schöll, J. Appl. Phys. **93**, 6347 (2003).
[43] T. Christen, Naturforsch. **49a**, 847 (1994).
[44] Here we negelect dependence of $T^{\star}$ and $T_{\star}$ on u, assuming $u = u_{\mathrm{co}}$. This does not change the results.
[45] J. Guckenheimer and P. Holmes, *Nonlinear Oscillations, Dynamical Systems, and Bifurcations of Vector Fields*, Applied Mathematical Sciences, Vol. 42 (Springer-Verlag, Berlin, 1983).
[46] K. Krischer and A. Mikhailov, Phys. Rev. Lett. **73**, 3165 (1994).
[47] C.P. Schenk, M. Or-Guil, M. Bode, and H.-G. Purwins, Phys. Rev. Lett. **78**, 3781 (1997).
[48] F.-J. Niedernostheide, M. Or-Guil, M. Kleinkes, and H.-G. Purwins, Phys. Rev. E **55**, 4107 (1997).
[49] H. Hempel, I. Schebesh, and L. Schimansky-Geier, Eur. Phys. J. B **2**, 399 (1998).
[50] M. Or-Guil, M. Bode, C.P. Schenk, and H.-G. Purwins, Phys. Rev. E **57**, 6432 (1998).
[51] M. Bode, A.W. Liehr, C.P. Schenk, and H.-G. Purwins, Physica C **161**, 45 (2002).
[52] F. Mertens, R. Imbihl, and A. Mikhailov, J. Chem. Phys. **101**, 9903 (1994).
[53] M. Falcke and H. Engel, J. Chem. Phys. **101**, 6255 (1994).
[54] M. Bertram and A. Mikhailov, Phys. Rev. E **67**, 036207 (2003).
[55] M. Bertram, C. Beta, M. Pollmann, A. Mikhailov, H. Potermund, and G. Ertl, Phys. Rev. E **67**, 036208 (2003).
[56] A.N. Zaikin and A.M. Zabotinsky, Nature (London) **225**, 535 (1970).
[57] E. Mihaliuk, T. Sakurai, F. Chirila, and K. Showalter, Phys. Rev. E **65**, 065602(R) (2002).
[58] B. Datsko, Fiz. Tekh. Poluprovodn. **11**, 250 (1996). [Semiconductors **31**, 146 (1997)].